

THE DORSA ARGENTEA FORMATION: SYNTHESIS OF GLACIAL FEATURES AND HISTORY OF LATE NOACHIAN-EARLY HESPERIAN MARTIAN CLIMATE CHANGE. K. E. Scanlon and J. W. Head III, Department of Geological Sciences, Brown University, Providence, RI, USA. <kathleen_scanlon@brown.edu>

Introduction: The Noachian and Hesperian-aged geomorphological units mapped [1-2] as the Dorsa Argentea Formation (DAF) and the Hesperian-Noachian undivided unit cover a combined area of $\sim 1.5 \cdot 10^6$ km² [3] surrounding and offset from the south pole of Mars. The units are characterized by sinuous and braided ridges, including the Dorsa Argentea for which the formation is named [e.g. 4-10], several regions of pitted terrain, the Cavi Angusti and Sisyphi Cavi [e.g. 11-13]; and steep-sided mountains, the Sisyphi Montes [e.g. 14]. A radar reflector closely correlated with the outline of the deposit is consistent with high concentrations of volatiles in and underlying the deposit [15].

In earlier work based on Mariner and Viking images, researchers proposed volcanic, tectonic, inverted stream, aeolian, and clastic dike origins for the Dorsa Argentea and other sinuous ridges (e.g., [1, 5]; see review in [3]) and widely agreed on an aeolian origin for the cavi [e.g. 11, 12]. Howard [4] was the first to propose a glacial origin for the deposit, wherein the sinuous ridges formed as eskers and the cavi formed from melt-out of ground ice. While the lack of other characteristic glacial landforms in the deposit was noted as a potential shortcoming of the glacial hypothesis [4], others noted that features previously interpreted to have arisen from aeolian scour could have been carved by ice streams [16]. MOLA topographic data showed that the Dorsa Argentea fulfilled the topographic criteria for esker identification [3] and that the depth and spatial relationships of the cavi were difficult to reconcile with an aeolian origin but consistent with an origin from volatile removal [3, 17], both of which further strengthened the glacial hypothesis.

In addition to the Dorsa Argentea and the cavi, since the Mars Global Surveyor mission numerous glacial and glaciofluvial features have been documented in the deposit (**Figure 1**). The Sisyphi Montes, which are aligned on the 0°W lobe of the DAF between $\sim 75^\circ$ S and 55° S, have high aspect ratios, steep sides, and in many cases flat tops, suggesting an origin from subglacial volcanism [14]; hydrated sulfates near the mountains may have originated in glaciovolcanic hydrothermal environments [18]. Fluvial channels and breached craters at the eastern margin of the 0°W lobe, near the Prometheus impact basin, indicate that melt-back of the DAF ice sheet produced at least 1000 km³ of meltwater over a short time [19]. At the opposite edge of the DAF, near Cavi Sisyphi and Cavi Angusti, large channels including Dzigai, Doanus, and Sirius Valles drain into the Argyre basin [e.g. 3, 20]. Pitted terrain, linear valleys, and smooth deposits adjacent to

Cavi Angusti and Argentea Planum have been interpreted as the remnants of a proglacial lake [3, 21].

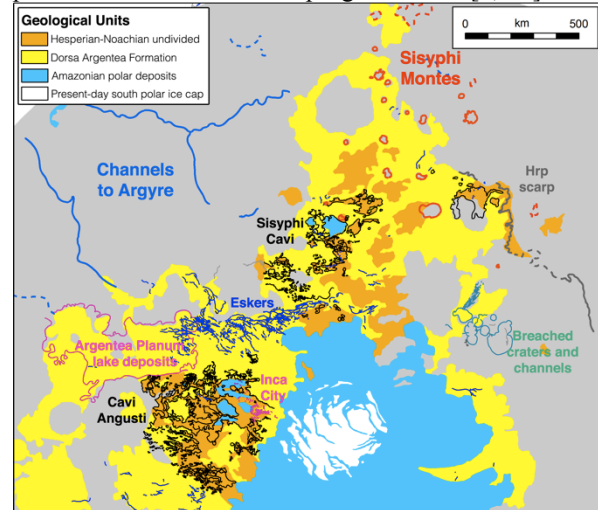


Fig. 1. Features interpreted to be of glacial origin in the Dorsa Argentea formation include cavi interpreted as melt-out terrains [e.g. 4, 13], lake deposits in Argentea Planum [3, 21], mountains whose morphology suggests a glaciovolcanic origin [e.g. 14], and fluvial channels connecting several craters [18]. The boundaries of the Dorsa Argentea formation, Hesperian-Noachian undivided terrain, Amazonian polar deposits, and present-day south polar cap are shown as mapped by Tanaka and Scott [1].

The DAF and Mars Climate History: The geomorphological evidence that a much more extensive south polar ice sheet was present in the late Noachian and early Hesperian adds to the evidence that the early martian climate was substantially different from the Amazonian climate. Notably, an extensive south polar ice sheet is a robust feature of ancient Mars climate simulations with a thicker atmosphere [22]. The offset of the DAF from the current south pole has been put forth as evidence for martian true polar wander caused by the formation of Tharsis [23]. In light of the geomorphological evidence for basal melting [e.g. 3, 10, 18, 21], the footprint of the deposit has also been used with glacial flow models to constrain the minimum temperature of the martian south polar region at the Noachian-Hesperian boundary [24].

In-depth geomorphological studies of glacial features in the unit, however, have thus far focused on detailing individual, spatially separated landform associations. To make use of the potential of the DAF as a key to the Noachian-Hesperian climate transition, we are mapping stratigraphic relationships between the glacial landforms in the DAF and using the relative timing of the ice sheet advance and retreat they record to synthesize a history of the DAF ice sheet as a whole. Under-

standing the nature of ice sheet growth and meltback recorded by the Dorsa Argentea Formation will provide insight into the nature of the Noachian-Hesperian climate transition: did temperatures decrease monotonically from a globally warmer climate where seasonal melting may have been possible near the equator? Does the DAF record any evidence for the hypothesized episodic, global warming that may have allowed the valley networks to form [e.g. 22, 25]? What were the relative contributions of volcanism and climate to the melting that carved fluvial landforms in the DAF?

We are also mapping contacts with non-glacial units nearby, including the Hesperian Ridged Plains that border the deposit. If the DAF is indeed glacial in origin, crater counting is not a reliable method for estimating the age of the units within it. Craters from impacts that occurred while ice was still present will be smaller than expected if they penetrated the ice cover, or will have been erased when the ice disappeared if they excavated only ice [e.g. 26]. Contacts with readily crater-dated features outside the deposits, such as lava flows, will allow us to circumvent this problem.

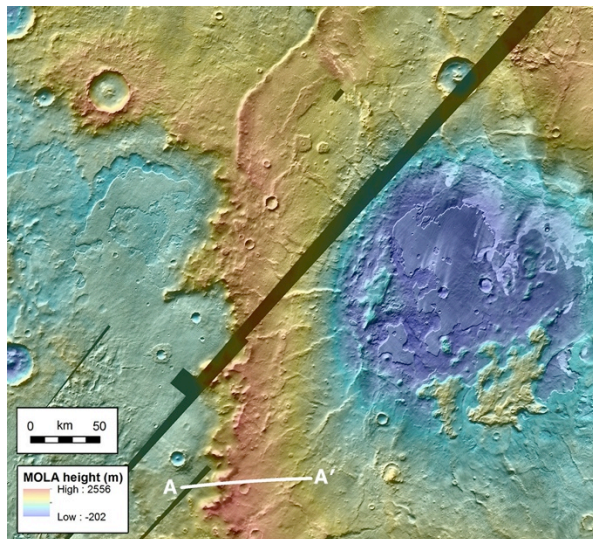


Fig. 2. Flows from Pityusa Patera steepen into a digitate, ~kilometer high scarp at the contact between Hesperian ridged plains and the Dorsa Argentea Formation, indicating that they chilled against the margin of the DAF ice sheet. THEMIS daytime IR image mosaic shaded with MOLA topography.

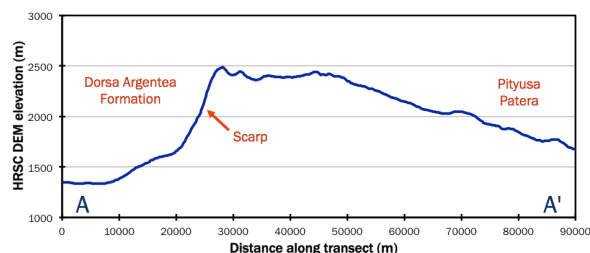


Fig. 3. MOLA topographic profile across the scarp (along the line A – A' in Figure 2).

The morphology of some contacts with other units provide further evidence for an ancient ice sheet in the DAF, and these contacts can be used to develop quantitative age / ice extent tie points for the Noachian-Hesperian history of the south pole. At the eastern edge of the 0°W lobe of the DAF, for example, the contact between the DAF and Hesperian Ridged Plains flows originating from the 3.8 ± 0.1 Ga edifice Pityusa Patera [27] is marked by a ~ 1 km high scarp (**Figures 2 and 3**). The steepness of the scarp and its digitate morphology in plan view are similar to scarps at the contacts between summit flows and the glacial fan-shaped deposits on each of the Tharsis Montes (**Figure 4**; [28, 29]) and we hypothesize that this scarp also formed by rapid chilling of flows that banked up against the Dorsa Argentea Formation ice sheet. The position of the scarp and the age of this flow demarcate the boundary of the DAF ice sheet at one point in time.

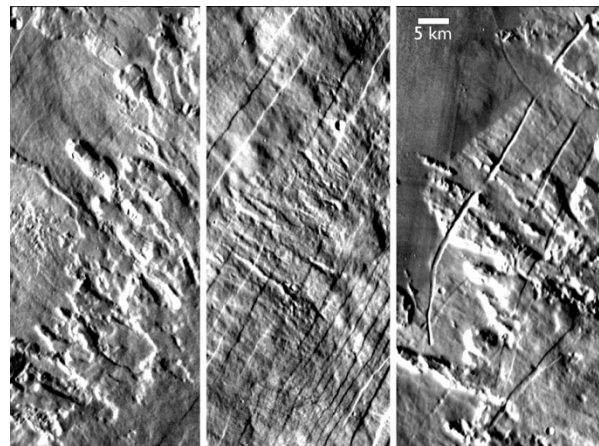


Fig. 4. Digitate flows at the upslope edge of the Arsia (left), Pavonis (center) and Ascræus Mons (right) fan-shaped glacial deposits [29].

References: [1] Tanaka, K.L., and D.H. Scott (1987), *USGS Map I-1802-C*. [2] Tanaka, K.L., and E.J. Kolb (2001), *Icarus*, 154, 3–21. [3] Head, J. W., and S. F. Pratt (2001), *JGR*, 106, 12275–12299. [4] Howard, A.D. (1981), *NASA TM 84211*, 286–288. [5] Ruff, S., and R. Greeley (1990), *LPI Tech. Report 90-06*, 253. [6] Head, J. W. (2000), *LPSC XXXI*, abstract #1116. [7] Head, J. W. (2000), *LPSC XXXI*, abstract #1117. [8] Head, J. W., and B. Hallet (2001), *LPSC XXXII*, abstract #1366. [9] Head, J. W., and B. Hallet (2001), *LPSC XXXII*, abstract #1373. [10] Kress, A., et al. (2010), *LPSC XLI*, abstract #1533. [11] Cutts, J. A. (1973), *JGR*, 78, 4211–4221. [12] Sharp, R. P. (1973), *JGR*, 78, 4222–4230. [13] Ghatan, G.J., et al. (2003), *JGR*, 108. [14] Ghatan, G.J., and J.W. Head (2002), *JGR*, 107. [15] Plaut, J.J., et al. (2007), *LPSC XXXVIII*, abstract #2144. [16] Kargel, J.S., and R.G. Strom (1992), *Geology*, 20, 3–7. [17] Ghatan, G.J., and J.W. Head (2004), *JGR*, 109. [18] Wray, J.J., et al. (2009), *Geology*, 37, 1043–1046. [19] Milkovich, S.M., et al. (2002), *JGR*, 107. [20] Parker, T.J. (1989), *LPSC XX*, 826–827. [21] Dickson, J.L., and J.W. Head (2006), *PSS*, 54, 251–272. [22] Wordsworth, R., et al. (2013), *Icarus*, 222, 1–19. [23] Kite, E. S., et al. (2009), *EPSS*, 280, 254–267. [24] Fastook, J.L., and J.W. Head (2012), *Icarus*, 219, 25–40. [25] Halevy, I., and J. W. Head (2012), *LPSC XLIII*, abstract #1908. [26] Kadish, S. J. et al. (2013), *PSS*, doi: 10.1016/j.pss.2013.12.005. [27] Williams, D. A., et al. (2009), *PSS*, 57, 895–916. [28] Kadish, S. J., et al., (2008), *Icarus*, 197, 84–109. [29] Scanlon, K.E., and J. W. Head (2013), *LPSC XLIV*, abstract #2091.